










TECHNICAL NOTE

Small extracellular vesicles derived from human adipose-derived mesenchymal stromal cells cultured in a new chemically-defined contaminate-free media exhibit enhanced biological and therapeutic effects on human chondrocytes in vitro and in a mouse osteoarthritis model

Hiroto Hanai¹  | David A. Hart²  | George Jacob³  | Kazunori Shimomura¹  |
Wataru Ando^{1,4}  | Yusuke Yoshioka⁵ | Takahiro Ochiya⁵  | Shinichi Nakagawa¹  |
Masato Nakamura¹ | Seiji Okada¹  | Norimasa Nakamura^{1,6,7} 

¹Department of Orthopaedic Surgery, Osaka University Graduate School of Medicine, Osaka, Japan

²Department of Surgery and the McCaig Institute for Bone & Joint Health, University of Calgary, Calgary, Canada

³Department of Orthopaedics, VPS Lakeshore Hospital, Kerala, India

⁴Department of Orthopaedic Surgery, Kansai Rosai Hospital, Hyogo, Japan

⁵Department of Molecular and Cellular Medicine, Institute of Medical Science, Tokyo Medical University, Tokyo, Japan

⁶Institute for Medical Science in Sports, Osaka Health Science University, Osaka, Japan

⁷Global Center for Medical Engineering and Informatics, Osaka University, Osaka, Japan

Correspondence

Norimasa Nakamura, Institute for Medical Science in Sports, Osaka Health Science University, 1-9 27, Tenma, Osaka City, Osaka, 530-0043, Japan.
Email: norimasa.nakamura@ohsu.ac.jp

Funding information

Japan Agency for Medical Research and Development, Grant/Award Number: JP22mk0101218; Japan Society for the Promotion of Science, Grant/Award Numbers: JP19H03781, JP22H03201

Abstract

Human small extracellular vesicles (sEVs) derived from adipose-derived mesenchymal stromal cells (ASC) have been reported to suppress the progression of osteoarthritis (OA) in animal studies and subsequently, translation of this potential to assess their clinical efficacy is anticipated. However, fabrication protocols for sEVs to eliminate potential contamination by culture medium-derived components need to be established prior to their clinical use. The purpose of the present studies was to elucidate the influence of medium-derived contaminants on the biological effects of sEVs, and to establish isolation methods for sEVs using a new clinical grade chemically-defined media (CDM). The quantity and purity of ASC-derived sEVs cultured in four different CDMs (CDM1, 2, 3 and 4) were evaluated. The concentrates of the four media incubated without cells were used as the background (BG) control for each set of sEVs. The biological effect of sEVs fabricated in the four different CDMs on normal human articular chondrocytes (hACs) were evaluated in vitro using a variety of methodological assessments. Finally, the sEVs with the highest purity were tested for their ability to suppress the progression of knee OA mouse model. Analysis of the BG controls revealed that CDM1-3 contained detectable particles, while there was no visible contamination of culture media-derived components detected with CDM4. Accordingly, the sEVs fabricated with CDM4 (CDM4-sEVs) exhibited the highest purity and yield. Notably, the CDM4-sEVs were the most efficient in promoting the cellular proliferation, migration, chondrogenic differentiation, and anti-apoptotic activity of hACs. Furthermore, CDM4-sEVs significantly suppressed the osteochondral degeneration in vivo model. Small EVs derived from ASCs cultured in a CDM without detectable contaminants demonstrated enhanced biological effects on hACs and the progression of OA. Thus, sEVs isolated with CDM4 most optimally meet the requirements of efficacy and safety for assessment in their future clinical applications.

This is an open access article under the terms of the [Creative Commons Attribution-NonCommercial-NoDerivs](https://creativecommons.org/licenses/by-nc-nd/4.0/) License, which permits use and distribution in any medium, provided the original work is properly cited, the use is non-commercial and no modifications or adaptations are made.

© 2023 The Authors. *Journal of Extracellular Vesicles* published by Wiley Periodicals, LLC on behalf of the International Society for Extracellular Vesicles.

KEYWORDS

adipose-derived mesenchymal stromal cells, chemically-defined media, exosomes, extracellular vesicles, human articular chondrocytes, osteoarthritis

1 | INTRODUCTION

Osteoarthritis (OA) is a degenerative disorder characterized by degradation of joint cartilage and bone triggered by a variety of insults to joint integrity and thus the term is an umbrella term for joint degeneration due to multiple causes (reviewed in Hart et al., 2021). However, progression of OA involves inflammation and a pro-inflammatory response of innate immunity (Woodell-May & Sommerfeld, 2020). It is estimated that 260 million people suffer from knee OA (KOA) worldwide with 12 million newly diagnosed, and thus this population is further increasing (James et al., 2018). Accordingly, the treatment of OA is a significant contributor to the global burden of medical costs (Gupta et al., 2005; Losina et al., 2015). Generally, treatment options for knee OA are limited; conservative therapies including physiotherapy and pharmacotherapy are attempted at early stages, however such treatment options often progress to major surgical treatments such as osteotomy and total knee arthroplasty (TKA) at the advanced stage of OA that accompanies malalignment of the lower extremity (OARSI White Paper- OA as a Serious Disease 2022). Recently, regeneration therapies have focused on biological restoration of articular surfaces. Specifically, cell therapy with mesenchymal stromal cells (MSCs) has been proposed (Lopa et al., 2019; Ng et al., 2020; Toh et al., 2014), with many human studies of intra-articular MSCs therapy for the treatment of KOA having been performed (McIntyre et al., 2018). Most trials reported varying levels of functional recovery without major adverse events and thus MSC-based therapy is emerging as a validated therapeutic option for the future.

Recently, a main mode of action of MSCs has been focused on their trophic effects (Caplan & Dennis, 2006; Hofer & Tuan, 2016; Maumus et al., 2013), including the promotion of cellular proliferation, chemo-attraction and anti-apoptosis effect (Maumus et al., 2013). The trophic activity of MSCs may be triggered by extracellular matrix (ECM) production, cell to cell contact or secretion of signaling molecules (Hofer & Tuan, 2016). Among the options, extracellular vesicles (EVs) derived from MSCs, especially exosomes, have emerged as one of the important components of MSC that mediate their effects (Katsuda & Ochiya, 2015). Extracellular vesicles are mainly classified as exosomes, microvesicles, and apoptotic bodies (Thery et al., 2018). These are often classified by size and developmental mechanism. For example, microvesicles are a population of membrane vesicles that are generated by outward budding or blebbing from the plasma membrane (Stahl et al., 2019). They range in size from 100 to 1000 nm and vary in shape. Apoptotic bodies are released exclusively from the plasma membrane during the late stages of apoptosis, and they range in size from 1 to 5 μm (Thery et al., 2001). These apoptotic bodies are somewhat comparable in size to platelets, and contain several intracellular fragments, organelles, membranes, and cytosolic contents. Whereas exosomes and microvesicles develop as a result of normal cellular processes with viable cells, apoptotic bodies occur only when programmed cell death occurs (Thery et al., 2001). An exosome is a vesicle with a diameter of approximately 100 nm and they are synthesized and released from multivesicular bodies that fuse with the plasma membrane by endocytosis (Doyle & Wang, 2019; Thery et al., 2018; Zaborowski et al., 2015). Exosomes are surrounded by a lipid bilayer and contain a cargo that includes various biomolecules, such as nucleic acids (miRNAs), proteins or lipids (Thery et al., 2018). It has been revealed that exosomes have an important role as mediators of cell-to-cell communication in that recipient cells take up the secreted exosomes and incorporate their cargo contents (Katsuda & Ochiya, 2015). Although exosomes released from cultured cells are known to exist in the culture media, it has been challenging to completely separate them from other vesicles, such as microvesicles, when collected (Thery et al., 2018). Therefore, extracellular vesicles mainly consisting of exosomes are operationally defined as small extracellular vesicles (sEVs) (Thery et al., 2018).

Several research studies regarding the therapeutic effects of MSC-derived sEVs (MSC-sEVs) have been undertaken in the field of musculoskeletal tissues (Cosenza et al., 2017; Woo et al., 2020; Zhang et al., 2018). The therapeutic potential of MSC-sEVs for cartilage injury or in osteoarthritis using mouse models have been reported (Cosenza et al., 2017; Zhang et al., 2018) and thus, future clinical applications of MSC-sEV-based therapies may emerge as a new cell-free therapy for the treatment of these conditions. To achieve such applications, optimization of purification methods for sEVs (Gowen et al., 2020; Kim et al., 2021) will be required to ensure their safety and efficacy. It is widely acknowledged that the gold standard for isolating sEVs from culture media in basic research is by ultracentrifugation (UC) (Thery et al., 2018). However, it is challenging to handle the media under clean operative circumstances and to obtain a high yield of sEVs using a single preparative method, circumstances which may ultimately be unrealistic in view of manufacturing requirements in clinical settings. In contrast, ultrafiltration (UF) using tangential flow filtration (TFF) or size-exclusion chromatography (SEC) followed by UF may be more appropriate in clinical settings (Gowen et al., 2020; Kim et al., 2021). Furthermore, contamination of culture media-derived materials should be avoided during the cell culture process to obtain pure, clinical grade MSC-sEVs. In this regard, it is preferable not to use fetal bovine serum (FBS) or human platelet lysate (hPL) containing media that could potentially also be a source of sEVs. Contamination of preparations with such sEVs may affect the proliferation ability and survival rate of MSCs (Li et al., 2015). Taken together, it is

desirable to culture the cells using a serum-free and xeno material-free chemically-defined media (CDM) to ensure the isolation of pure sEVs to meet Good Manufacturing Practice (GMP) requirements during the whole fabrication process.

The goal of the present study was to establish the most optimal conditions for obtaining clinical-grade pure sEVs from adipose-derived mesenchymal stromal cells (ASCs) which retain maximal biological effect. We compared the results obtained with four different xeno- and serum-free CDMs that could be used in the sEVs fabrication process and characterized the amount and purity of isolated sEVs released from ASCs. We further tested the effect of the sEVs using the four different CDMs on cellular proliferation, migration, chondrogenic differentiation, and apoptosis of normal human articular chondrocytes (hACs). We hypothesized that the isolated sEVs with highest purity would most efficiently affect cellular activities. Finally, the best sEVs preparations, based on the results from the *in vitro* assays were tested for their efficacy to suppress the progression of joint destruction using a mouse osteoarthritis model.

2 | MATERIALS AND METHODS

Prior to the reported experiments being performed, the approval of the Institutional Committee for Medical Ethics and the Institutional Animal Care and Use Committee was granted (authorization number; 14102-9 and 01-001-004, respectively).

2.1 | Culture of ASCs

Human ASCs were selected as the source of sEVs in this research as they have been already used for the clinical treatment of osteoarthritis (Yokota et al., 2019). ASCs were obtained via liposuction aspirate from abdominal subcutaneous adipose tissue of donor patients ($N = 3$) and used after expansion by culturing the MSC as previously described (Yokota et al., 2019). Briefly, after several washing with Ringer's lactate solution (Fuso Pharmaceutical Industries, Osaka, Japan), adipose tissue was digested with collagenase and thermolysin (Both from Amano Enzyme, Aichi, Japan) for 45 min at 37°C. The cells were obtained from digested tissue by centrifugation, and were then seeded on plastic culture dishes in the expansion medium, consisted of DMEM/F-12 (Wako pure Chemical, Osaka, Japan) supplemented with NeoSERA (Japan Biomedical, Hokkaido, Japan) and Human Recombinant basic fibroblast growth factor (bFGF, REPROCELL, Kanagawa, Japan). Passage 2–4 cells were used for all experiments. To confirm the success of ASC isolation as a MSC, ASCs were analyzed regarding their tri-lineage differentiation potential and their surface marker phenotype, based on the guidelines of the International Society for Cellular Therapy (ISCT) (Dominici et al., 2006). The methods used for evaluating MSC characteristics are described in the Supplemental information file. Normal human articular chondrocytes (hACs) were purchased from Lonza (CC-2550, Morristown, NJ, USA) and cultured according to the manufacturer's protocol. All cells were cultured in a humid incubator at 37°C in 5% CO₂ and medium was changed twice a week.

2.2 | ExoScreen assay

Four different xeno- and serum-free CDMs were used for the extraction and purification process for the sEVs comparisons. CDM1 (KBM ADSC4, KOJIN BIO, Saitama, Japan) (cited 2022 July 6th), CDM2 (MSC NutriStem XF, Sartorius, Göttingen, Germany) (Lisini et al., 2019) and CDM3 (StemPro MSC SFM XenoFree, Gibco, Carlsbad, CA, USA) (Lindroos et al., 2009) are commercially available GMP-compliant, serum-, xeno-, and phenol red-free media. CDM4 is newly developed GMP-compliant, serum-, xeno-free media developed with the goal of avoiding contamination by unknown substances in the purified sEVs using an ultrafiltration method (Japanese Patent Application No. 2022-154219, CellSource, Tokyo, Japan).

ExoScreen assays were performed to evaluate the quantity of sEVs in the culture supernatant, which is an ultra-sensitive method for exosome evaluation developed by Yoshioka et al. (2014). Briefly, ASCs were seeded in expansion media on 96 well plates at 7500 cells/well on day 0. At day 2 of culture, the medium was aspirated, the cells washed with sterile PBS, and the media changed to 100 μ L of each CDM (CDM 1–4). Fifty microliters of each medium-specific supernatant were collected after 24 and 48 h. Subsequently, 25 μ L of each collected sample was exposed to 5 nM biotinylated monoclonal anti-human CD9 or CD63 antibodies (Cosmo Bio, Carlsbad, CA, USA) and 50 μ g/mL AlphaLISA acceptor beads (PerkinElmer, Waltham, MA, USA) conjugated with anti-human CD9 or CD63 antibodies (Cosmo Bio) and were placed into 96 well half-area white plates. After a 3 h incubation at 37°C in the dark, 25 μ L of 80 μ g/mL AlphaScreen streptavidin-coated donor beads (PerkinElmer) were added and the mixture incubated for an additional 1 h. Plates were then assessed on an EnVision (PerkinElmer) using the AlphaScreen measurement mode. The signal intensity of a PBS sample was subtracted as a background value from the experimental values. Also, to correct for the number of cells, 50 μ L of the remaining medium from the cell-culture wells after the sample collection for ExoScreen assays were stained using a Cell Counting Kit-8 (CCK-8, Dojindo, Kumamoto, Japan) by adding 50 μ L of the medium and 10 μ L of the reagent and the resulting absorbance was quantified according to the protocol. The indicated wavelengths were assessed using a Multiskan GO (Thermo Fisher Scientific, Carlsbad, CA, USA).

2.3 | Extraction and purification of sEVs

When ASCs had expanded to 80% confluency, the medium was changed to each CDM after washing the cells with PBS. After culturing for another 2 days, each supernatant was collected and centrifuged at $2000 \times g$ for 10 min at 4°C to deposit any debris. Subsequently, the resulting supernatant was subjected to filtration through a $0.22\text{-}\mu\text{m}$ filter and stored at 4°C until the next extraction step. Each conditioned culture media sample was then further extracted by the tangential flow filtration system. Each sample was concentrated approximately 10-fold by filtering through 100 kDa membranes and the same process was repeated three times by adding PBS for washing to ultimately obtain the sEVs. For studies of extracellular vesicles (MISEV), 2018 guidelines suggest that it is desirable to use a sample isolated from non-conditioned medium without cell culturing as a negative control comparator for evaluating the properties of conditioned media-derived sEVs (Thery et al., 2018). Accordingly, the concentrates from each non-conditioned CDM were prepared as a background control (BG) using the same process as was used for the isolation of the conditioned CDM-derived sEVs. The corresponding EV and BG were prepared at the same enrichment ratio. Preparations were stored at 4°C for less than one month before being used for the reported experiments.

2.4 | Nanoparticle tracking analysis (NTA)

Nanoparticle concentrations and size distributions were determined using a NanoSight LM10 or NS300 (Malvern, Worcestershire, UK) as previously described (Yoshioka et al., 2014). Samples were diluted to the optimal concentration (40–100 times) using contamination-free PBS and a 60-s video was captured. The camera level was set at 14 and the detection threshold was 7. In addition, protein concentrations were measured using a Qubit Protein Assay Kit and a Qubit Fluorometer (Invitrogen) according to the manufacturer's instructions. When the particle count was less than 20 particles/frame for NTA or the protein concentration was out of range on Qubit, the outcomes were defined as not detected (ND).

2.5 | Silver staining

Protein distribution in each sample subjected to electrophoresis were visualized by silver staining according to a previous study (Hanai et al., 2020). Samples adjusted to 500 ng of protein with RIPA buffer (Thermo, Carlsbad, CA, USA) were mixed with loading buffer (NuPAGE, Thermo) and reduced using dithiothreitol (DTT). Components were separated using 4%–12% Bis-Tris gel (Thermo) by electrophoresis in MOPS running buffer (Thermo) for 40 min at a constant 200 V. For comparison, BG samples at the same volume as the corresponding EV and bovine serum albumin (BSA, Sigma-Aldrich, St. Louis, MO, USA) at the same protein quantity were also subjected to electrophoresis. A Silver Stain Kit II (Wako) was used to stain the gels according to the manufacturer's protocol and the stained gels were photographed using Chemi Doc Touch (Bio-Rad, Hercules, CA, USA).

2.6 | Transmission electron microscope (TEM)

The TEM assessment of sEVs was outsourced to Hanaichi UltraStructure Research Institute (Aichi, Japan). Briefly, samples were loaded onto carbon film supported copper grids with a 400 mesh, fixed and washed followed by contrasting with 2% uranyl acetate and then observed using TEM (H-7600, HITACHI, Tokyo, Japan) after air-drying. Each CDM-derived sEVs was pre-diluted by 5-fold. Observation magnification was $10,000\times$.

2.7 | Western blotting and enzyme-linked immunosorbent assay (ELISA)

Gels were prepared using the same method as for silver staining except for the reducing or non-reducing conditions; DTT was mixed for calnexin and albumin, and not for CD9, CD63 and CD81 (Hanai et al., 2020; Yoshioka et al., 2014). Cell lysates of ASCs were collected in RIPA buffer and loaded at a 5-fold higher protein level than for that of each EV sample. Depending on the target protein to be assessed, the loading amount was adjusted keeping the same protein ratio. After transfer to the PVDF membrane, they were blocked with Blocking One (Nacalai Tesque, Kyoto, Japan) for 1 h. The membranes were incubated with primary mouse monoclonal anti-human antibodies against CD9 (1:2000), CD63 (1:500), CD81 (1:1000) (all from Cosmo Bio), and a rabbit polyclonal antibody to albumin (1:40000, Proteintech, Rosemont, IL, USA) in Can Get Signal Solution 1 (Toyobo, Osaka, Japan) overnight at 4°C . Subsequently, they were incubated with secondary IgG horseradish peroxidase (HRP) conjugated antibodies against mouse or rabbit (both 1:20,000 dilution from Biocompare, South San Francisco, CA, USA) in Can Get Signal Solution 2 for 1 h at room temperature. Protein expression was detected using ImmunoStar LD (Wako). The amount of sEVs in each EV samples was measured using a CD9/CD63 Exosome ELISA Kit for Human (Cosmo Bio) according to the manufacturer's instructions. The CD9/CD63 fusion protein that came with the kit was used for the calibration curve.

2.8 | Colorimetric nanoplasmonic assay

A colorimetric nanoplasmonic assay was also utilized to determine sample purity. Based on the report of Maiolo et al. (2015), the test samples for sEVs were diluted 4 fold with PBS and then mixed with 6 nM gold nanoparticles (15 nm, Cytodiagnostics, Ontario, Canada) at a volume ratio of 2:1. After a 20 min incubation at room temperature, the mixtures were transferred to a cuvette and the UV–vis spectra between 400 and 800 nm were measured. The test sample was replaced with PBS as a negative control or 0.2% w/v of BSA for a positive control.

2.9 | Cell proliferation assay and cell migration assay

Three thousand hACs were seeded onto 96 well plates on day 0. After overnight incubation, the medium was changed to high glucose DMEM with 2% exosome-depleted FBS (Gibco) and 1% Antibiotic Antimycotic Solution (AA, Sigma) and each sample of sEVs, BG or vehicle control (PBS) was added at a concentration of 5×10^9 particles/mL for each of the EV group elements or at an equivalent volume for each of the BG or control groups. The absorbance was measured using CCK-8 on day 4 and 7 as previously described (Woo et al., 2020). The influence on migration of hACs was assessed using a CytoSelect Cell Migration Assay kit (Cell Biolab, San Diego, CA, USA) as previously described (Woo et al., 2020). Briefly, 1.5×10^5 of hACs in serum-free DMEM with 1% AA were seeded into the upper chamber and each sample in DMEM with 0.1% exosome-depleted FBS and 1% AA was added into the lower chamber at a concentration of 5×10^9 particles/mL for each of the EV group elements or at an equivalent volume for each of the BG or control groups. After an 8 h incubation, cells on the underside of the membrane with 8 μ m pore size were stained with the staining buffer and the number of migrated cells were counted using three randomly selected visualized fields at 10 \times magnification.

2.10 | Gene expression analysis

hACs were cultured as a micromass (1×10^5 cells in 10 μ L) on 12 well plates to evaluate ECM synthesis ability as described previously (Tateiwa et al., 2022). After a 3 h incubation, the chondrogenic basal media and each of the EV, BG sample or vehicle control (PBS) were added. Chondrogenic basal media consisted of DMEM with high glucose (Nacalai), 50 μ g/mL L-ascorbic acid, 40 μ g/mL L-proline (Wako), 1% ITS+ Premix (Corning, New York, NY, United States) and 1% AA, and each sample of sEVs, BG or vehicle control was added at a concentration of 5×10^9 particles/mL for each of the EV group elements or at an equivalent volume for each of the BG or control groups. After 2 days of incubation, cell masses were collected by QIAzol (Qiagen, Hilden, Germany). RNA was isolated by Direct-zol RNA Microprep kit (Zymo Research, Irvine, CA, United States) and cDNA was synthesized by using ReverTra Ace qPCR RT Master Mix with gDNA Remover (Toyobo) as described previously (Hanai et al., 2020). Gene expression (COL1A1 and COL2A1) was assessed by real-time PCR on a Step One Plus system (Applied Biosystems, Carlsbad, CA, USA). Beta-actin (ACTB) was used as an internal control gene for normalization and relative gene expression was calculated with the $2^{-\Delta\Delta CT}$ method. Primer sequences are listed in Table S1.

2.11 | Apoptosis assay

Twenty-four well plates were filled with 1×10^5 hACs/well and incubated overnight. The medium was changed to serum-free DMEM for apoptosis induction and each sample was added at a concentration of 5×10^9 particles/mL for each of the EV group elements or at an equivalent volume for each of the BG or control groups. After another 24 h incubation, cells were collected and incubated with Annexin-V APC (Biolegend) and 7-AAD (7-Amino-ActinomycinD, BD Biosciences, Franklin Lakes, NJ, USA) for 15 min at room temperature in the absence of light as described previously (Huang et al., 2018). Fluorescently labeled cells were analyzed by flow cytometry and the percentage positive for Annexin-V (+) 7-AAD (–) cells were defined as being in early apoptosis, was calculated.

2.12 | Collagenase induced osteoarthritis (CIOA) model mouse

All animals were housed under a 12-h dark–light cycle at room temperature with water and food freely available. CIOA was induced in the knee of 8-week-old C57BL/6 male mice. The CIOA model in mice has been established as a model for the pharmacological evaluation of OA (Kuyinu et al., 2016; Maumus et al., 2016). Sixteen mice were injected with 1 U of collagenase VII (Sigma) in 8 μ L PBS percutaneously into the right knee joint under anesthesia on day 1. They were randomly assigned to two

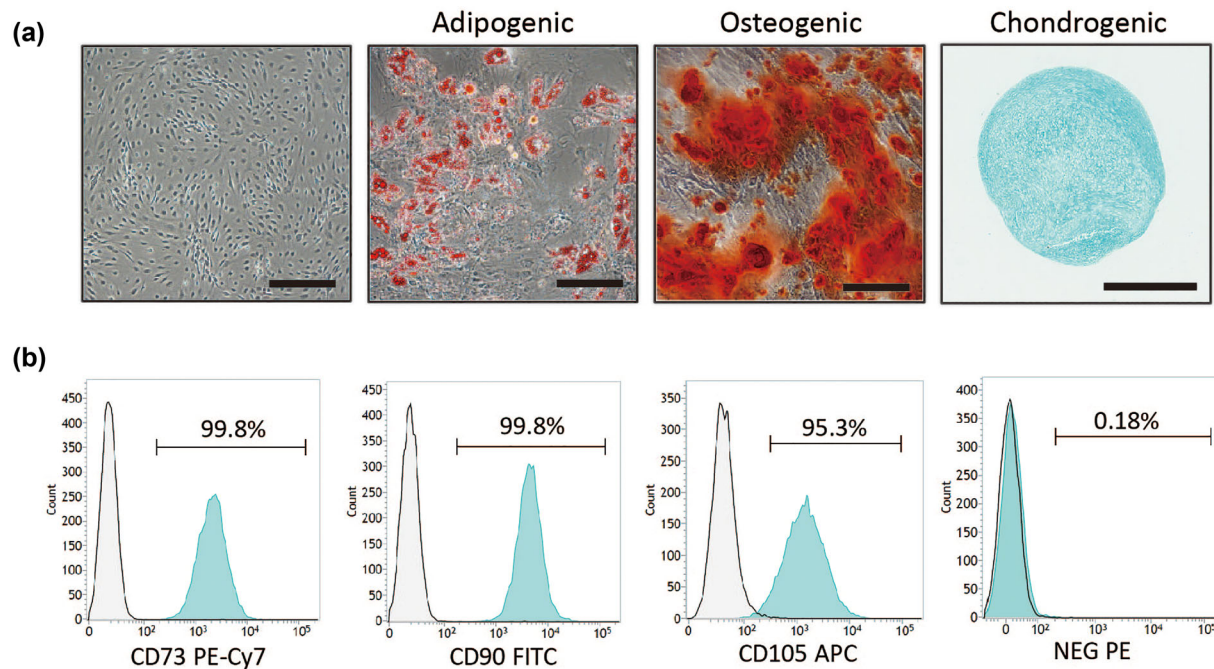


FIGURE 1 Characteristics of ASC as MSC. (a) Microscopic images of ASCs showing their fibroblast-like shape, and tri-lineage differentiation potential to the adipogenic, osteogenic and chondrogenic (stained with Oil Red, Alizarin Red and Alcian Blue, respectively) lineages. Scale bar: 500 μm . (b) Flow cytometry analysis of surface markers. Colored histograms correspond to test samples stained with each fluorescent marker and black lines correspond to control samples stained with each isotype. NEG means the antibody cocktail of CD11b, CD19, CD31, CD45 and HLA-DR known as MSC negative markers. The percentage indicates the ratio of the positive events to all events in the tested sample.

groups on day 8 and the treated group received 1×10^9 in 8 μL of sEVs, while the control group received the equivalent volume of BG.

Mice were sacrificed on day 28 and their tibias were collected. Randomly selected five contralateral tibias were used as normal controls. The articular surface of the tibia was observed macroscopically and assessed using a chondropathy scoring system for knee joints based on the Guingamp classification (Guingamp et al., 1997). Scores are assigned from 0 (normal) to 4 (worst) (Table S2). The medial and lateral tibial plateau were scored separately, and the total scores were used to obtain a final score. Subsequently, the tibia bone samples were fixed in formalin and demineralized with EDTA after serial dehydration with ethanol. After paraffin fixation, sections of the central part of the tibia in the coronal aspect was prepared with 3 μm thickness. The sections were stained with safranin O and the medial aspect of the tibia was evaluated using the Osteoarthritis Research Society International (OARSI) semi-quantitative scoring system (Glasson et al., 2010). Scores were assigned from 0 (normal) to 6 (worst) (Table S3).

2.13 | Statistical analysis

Data are expressed as the mean \pm standard deviation (SD) or a box plot. Not detected (ND) data was assigned as a 0 in the statistical analysis. Student's *t*-test for two-group comparisons and ANOVA for multiple-group comparisons followed by post-hoc analyze of Tukey–Kramer test for in vitro data and Steel–Dwass test for in vivo data were performed using JMP pro 14.0.0 (SAS Institute, Cary, NC, USA) and the significance was set as $p < 0.05$.

3 | RESULTS

3.1 | Characterization of ASC as MSC

During culturing on plastic dish, ASCs maintained their fibroblast-like spindle morphology and subsequently their ability to differentiate into adipocytes, osteoblasts and chondroblasts was confirmed (Figure 1a). According to flow cytometry analysis, the ASC exhibited >95% positive expression for CD73, CD90 and CD105, while the corresponding expression of a negative marker cocktail, which consisted of mixture detecting CD11b/CD19/CD31/CD45/HLA-DR, was <2% (Figure 1b).

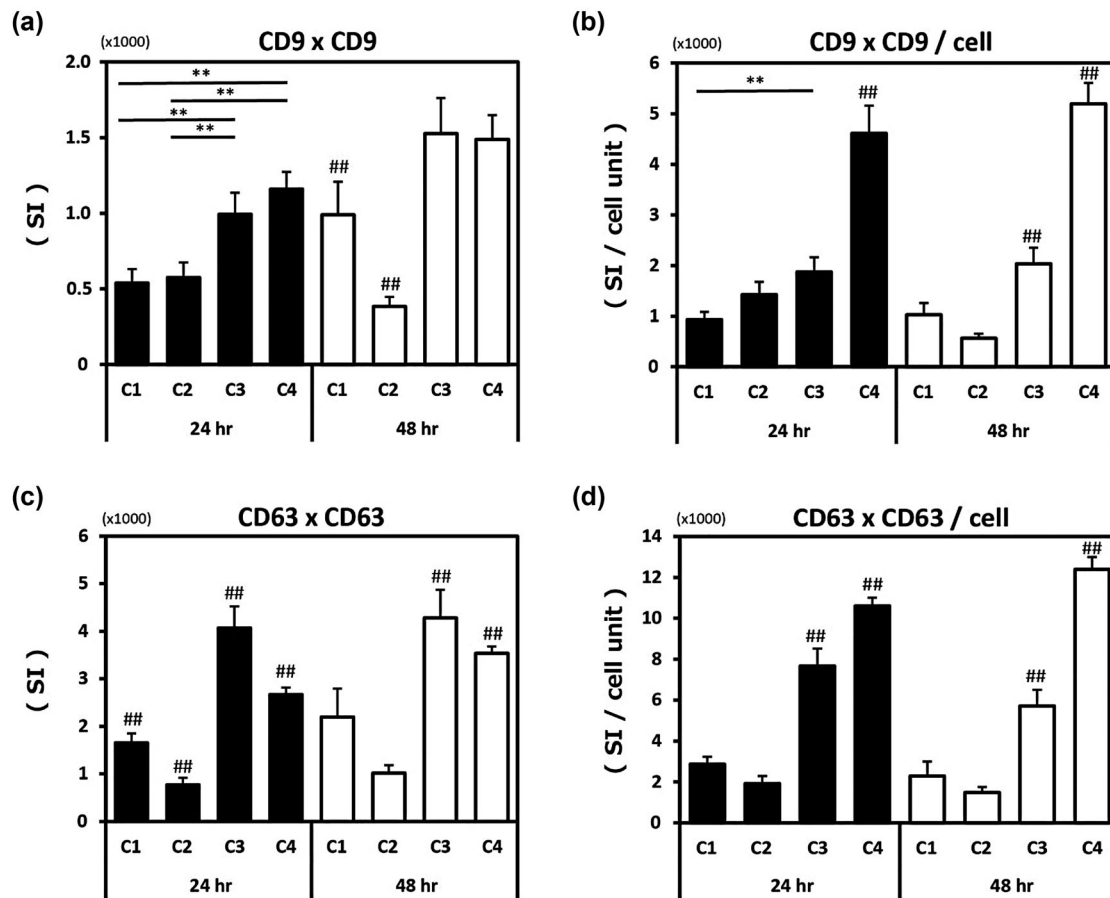


FIGURE 2 ExoScreen assay for the quantification of sEVs released into the culture media. ASCs were cultured in each of the indicated medium for 24 or 48 hr and the supernatants were analyzed on ExoScreen assay. (a, b) Signal intensity (SI) of CD9 x CD9 sEVs at 24 or 48 hr and the collected data by cell units. (c, d) SI of CD63 x CD63 sEVs at 24 or 48 hr and the collected data. $n = 5-6$. **, #: $p < 0.01$, as compared between two groups connected by a bar or to the other groups, respectively. C1 to C4 correspond to CDM1 to CDM4, respectively.

3.2 | The quantity of secreted sEVs in different culture media

To assess the quantity of sEVs released into each culture medium before the isolation process, the quantification of CD9 or CD63 positive sEVs was evaluated by the ExoScreen method. Small vesicles sandwiched between biotinylated anti-CD9 antibodies and AlphaLISA acceptor beads conjugated with anti CD9 antibodies (CD9 x CD9) were detected as luminescent signals triggered by the excitation of the AlphaScreen streptavidin-coated donor beads (Figure 2a, b). Each culture medium sample contained CD9 positive sEVs and when the samples collected at the 24 h timepoint were compared, the CDM4 and CDM3 groups contained significantly more sEVs than did the CDM1 and CDM2 groups ($p < 0.01$), and a similar pattern was observed for the 48 h samples (Figure 2a). Because of the different proliferative capacity provided to the cells by each medium, when corrected for the number of cells in each medium at each time point the CDM4 group contained significantly higher numbers of CD9 positive sEVs than did the other samples at any of the time points assessed ($p < 0.01$) (Figure 2b). The number of CD63 positive sEVs detected was significantly higher in the CDM3 group than in the other groups at both 24 and 48 h ($p < 0.01$). However, after correction for cell number the CDM4 group contained significantly higher numbers of CD63 positive sEVs at both time points ($p < 0.01$) (Figure 2c, d). Taken together, the CDM4 media most efficiently enhanced the release of sEVs from ASCs.

3.3 | Evaluation of the purity of sEVs isolated from the different CDM sources

Each conditioned media-derived sEV preparation and the concentrates from each culture-free medium (BG) were purified using the TFF system. All sEV samples contained some non-EV particles as determined by images captured from NTA (Figure 3a, Supplemental file S1). Notably, the BG samples for CDM 1, 2 and 3 also contained particles whose peak of distribution was approximately 80–140 nm in diameter and thus were in the media but were not associated with any ASCs. Conversely, there were

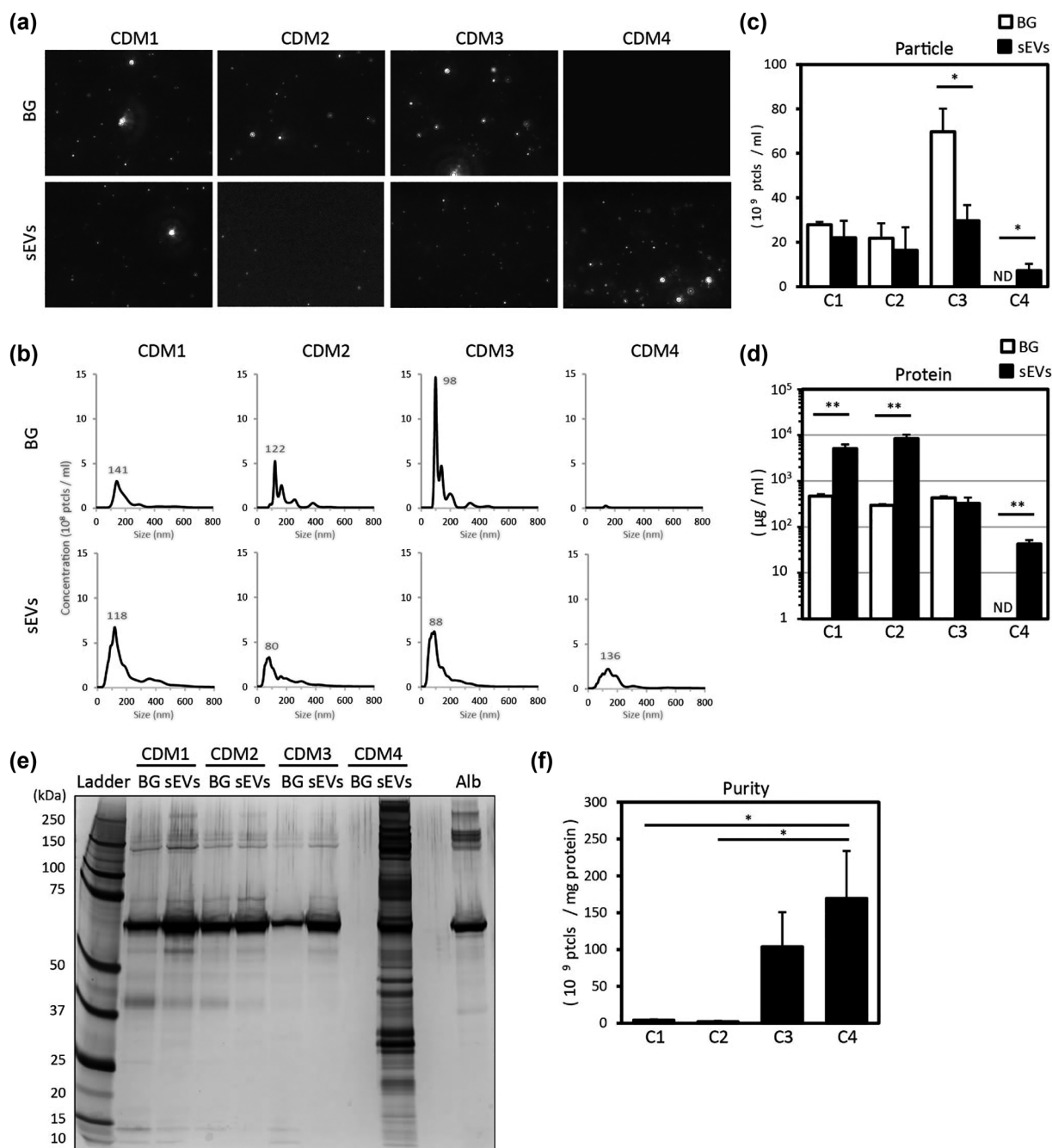


FIGURE 3 Distribution of the particles and proteins from sEVs and BG isolated from the different medium sources. Each cultured medium-derived sEVs and the concentrates from each culture-free medium (BG) were extracted and compared. (a, b) The representative captured images of particles and histogram of size distribution detected by NTA. (c, d) The data of the particle concentration and protein concentration of each sample. (e) Protein distribution by silver stain. Alb: albumin. (f) Purity data of each cell cultured medium-derived sEVs group calculated as the particles numbers per proteins. ND (not detected) indicates that the particle count was less than 20 particles/frame or the protein concentration was out of range and is designated with a 0 for the statistical analysis. $n = 3$. *: $p < 0.05$, **: $p < 0.01$, as compared between two groups connected by a bar. C1 to C4 correspond to CDM1 to CDM4, respectively.

no detectable particles in the BG sample for CDM4 (Figure 3b). When comparing the particle concentration between each of the sEVs and the BG, there were no significant differences detected for the CDM1 and 2 groups (Figure 3c). The CDM3-sEVs had significantly fewer particles than did the CDM3-BG group ($p < 0.05$). Conversely, the CDM4-sEVs had significantly more particles than the CDM4-BG group as the latter group had no detectable non-EV particles ($p < 0.05$).

The protein concentrations were assessed as an indicator of potential contamination of the EV samples (Figure 3d). The values were significantly higher in the EV compared to the BG groups for CDM1, 2 and 4 groups ($p < 0.01$), but no significant differences were observed for the CDM3 group ($p = 1.0$). Notably, there was no detectable protein concentration for the CDM4-BG group,

also consistent with the inability to detect non-EV particles reported above. To confirm the protein content in each sample, gel staining after electrophoresis was performed (Figure 3e). A major band in both the BG and EV samples for the CDM1, 2 and 3 groups were detected at 60–70 kDa, similar to the apparent molecular weight for the reference albumin (detected at 66 kDa). This suggests that a major protein contained in these samples may be albumin which presumably was added to the media prior to purchase, and is associated with the BG particles. In contrast, as presented in Figure 3d, no protein bands were detected in the CDM4-BG lane after electrophoresis (Figure 3e). Unlike the other sEVs samples in the CDM 1, 2 and 3 groups, a wide range of protein bands were detected in CDM4-derived sEVs, suggesting the presence of a variety of proteins. These band patterns were similarly detected with cells from three different donors (Figure S2). Also, as estimate of the purity of the sEVs samples was calculated by dividing particle concentration by the protein concentration. The purity of the CDM4-sEVs was highest as compared with that of the CDM1, 2 and 3-sEVs groups (Figure 3f).

3.4 | Comparison of TEM images, sEVs markers, nanoplasmonic assay between each cell cultured media derived EV

TEM captured the particles of approximately 50–100 nm in diameter and with a membrane structure in all sEVs groups, but many rod-shaped impurities were detected especially in the CDM1, 2 and 3-sEVs groups (Figure 4a). To assess the presence of exosomes in each sEVs group, the expression of classical exosome positive and negative marker proteins was examined. CD9, CD63 and CD81 expression could be detected only with the CDM4-sEVs by Western blotting, which was 5 times more concentrated than for the ASC lysates, when compared on the basis of their protein content (Figure 4b). On the other hand, calnexin, which is known as a component of the ER and serves as a negative marker for EV (Thery et al., 2018), was not detected in all sEVs groups. In contrast, the CDM1, 2 and 3-sEVs groups contained higher albumin levels than did the CDM4-sEVs. When compared on the basis of sample volume, CD9 and CD63 positive substances (which was identical to sEVs) could be detected in all groups by ELISA (Figure 4c). The mean value for the CDM4-sEVs was the highest but no significant differences between groups were detected ($p = 0.06$). However, when these values were converted to per-protein values, CD9 and CD63 positive sEVs in the CDM4-sEVs were about 17 to 570 times higher than the other CDM-sEVs with significant differences detected ($p < 0.01$) (Figure 4d). The CDM4-sEVs were also 4–16 times higher than the other CDMs when numbers were converted to per-particle values ($p < 0.05$) (Figure 4e).

Nanoplasmonic assays were also performed to determine the purity of each sEVs sample by assessing the interaction of gold nanoplasmonics, proteins with lipid membranes (Figure 4f–h). To explain briefly, the color of the solution turns to blue from red when EVs in PBS are added to the reagent, while the solution retains the initial red color when many single and aggregated exogenous proteins are added (Maiolo et al., 2015). Visually, the CDM1 and 2-sEVs yielded a color similar to the albumin control. On the other hand, the color of the CDM4-sEVs-assessed liquid changed from red, which was also different from the response of the PBS control. The color resulting with the CDM3-sEVs was intermediate, which was different from the colors for either the CDM1 and 2-sEVs or the CDM4-sEVs (Figure 4f). A similar pattern was observed for the spectrum analysis (Figure 4g). The values for the CDM4-sEVs were significantly lower than those for the albumin control and the other groups tested ($p < 0.01$). Values for the CDM-sEV 1–3 samples were significantly higher than the PBS control ($p < 0.01$) for the aggregation index (AI), which is presented as the ratio of the wavelength at 540 and 650 nm values (Figure 4h). Taken together, the CDM4-sEVs samples appear to be the purest of all the samples assessed with respect to the relationship between the particles with a lipid membrane as a sEV and exogenous protein.

3.5 | Evaluation of the influence of sEVs and BG on articular chondrocytes in vitro

To evaluate the influence of sEVs on human articular chondrocytes (hACs), each sample of sEVs, BG or vehicle control (PBS) was added at a concentration of 5×10^9 particles/mL for each of the EV groups or at the equivalent volume for each of the BG or control groups. Proliferation of human ACs was significantly enhanced following addition of the medium-derived EV compared to control (PBS) values on day 3 ($p < 0.01$, except for the CDM2-sEVs: $p < 0.05$) (Figure 5a). A significant proliferative effect was also observed following addition of each uncultured CDM-derived BG except for the CDM4-BG, compared to the PBS control group ($p < 0.01$, except for the CDM3-BG: $p < 0.05$). Only with the CDM4 series of additions was a proliferative effect promoted by adding the sEVs with a significant difference noted when compared to the BG ($p < 0.01$). At day 7, only in the CDM4 series did the sEVs maintain the promotion of the proliferative capacity of the hACs, with significant differences when compared to both the BG and the PBS control group ($p < 0.01$). There were no significant differences between the BG and the PBS control groups detected ($p = 1.0$). The migration capacity of hACs was also significantly enhanced with addition of every CDM-derived sEV group as compared with the corresponding BG group or the PBS control group ($p < 0.01$) (Figure 5b, c). The CDM1, 2 and 3-derived BG groups also gave rise to significant changes compared to the PBS control group ($p < 0.01$), but only the CDM4-BG group showed no significant difference in comparison with the PBS control group ($p = 0.98$).

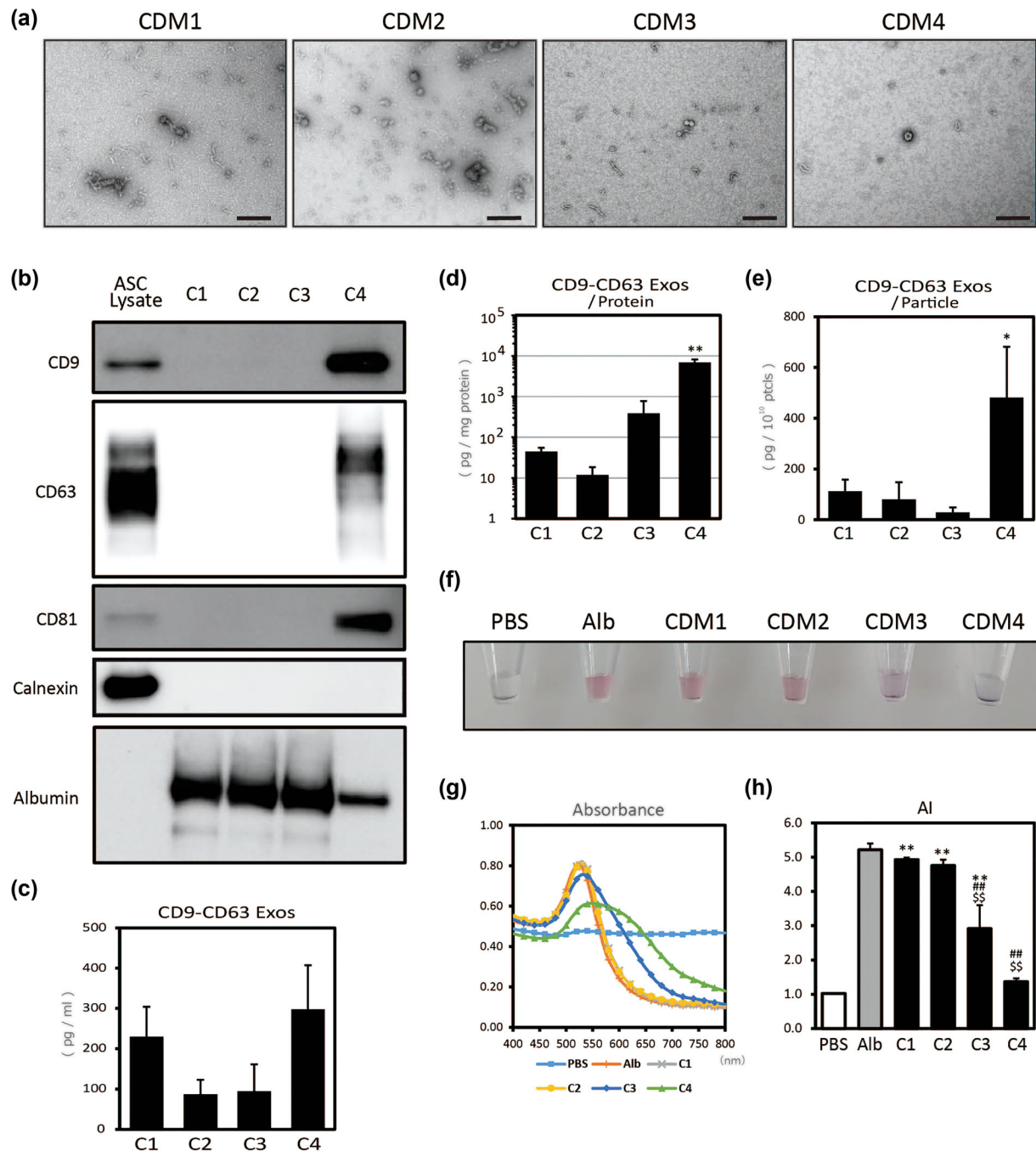


FIGURE 4 Assessment of TEM images, exosome markers, and nanoplasmonic assays for sEVs derived from each cell culture medium. (a) Representative TEM images. (b) Assessment of classical exosome positive and negative marker proteins and albumin by Western blotting. (c) Quantification analysis of sEVs for CD9-CD63 as measured by ELISA. The values were calculated using the CD9/CD63 fusion protein as a standard. (d, e) The adjusted data of CD9-CD63 positive sEVs by protein or particle numbers. $n = 3$. *: $p < 0.05$, **: $p < 0.01$, as compared to other groups. (f-h) The representative visualized solution color, the representative spectrum of the absorbance and the aggregation index (AI) by colorimetric nanoplasmonic assay. $n = 3$. **, ##, \$\$: $p < 0.01$, as compared to the PBS control, the albumin (Alb) control or other tested groups, respectively. C1 to C4 correspond to CDM1 to CDM4, respectively.

A similar trend was observed for the synthesis of ECM and anti-apoptosis activity by hACs (Figure 5d-f). The gene expression levels for COL1A1 and COL2A1 by hACs were significantly enhanced with the CDM4-sEVs samples compared to the corresponding BG and the PBS control groups ($p < 0.01$, except for the CDM4-BG vs. the CDM4-sEVs for COL1A1: $p < 0.05$) (Figure 5d). The CDM4-BG group also exhibited no significant differences when compared with the PBS control group results ($p = 0.68$ for COL1A1 and 0.93 for COL2A1). In the CDM1 series, the BG group resulted in significant enhancement of ECM synthesis when compared to the sEVs group results ($p < 0.01$). The early apoptosis induced in hACs was significantly suppressed in the

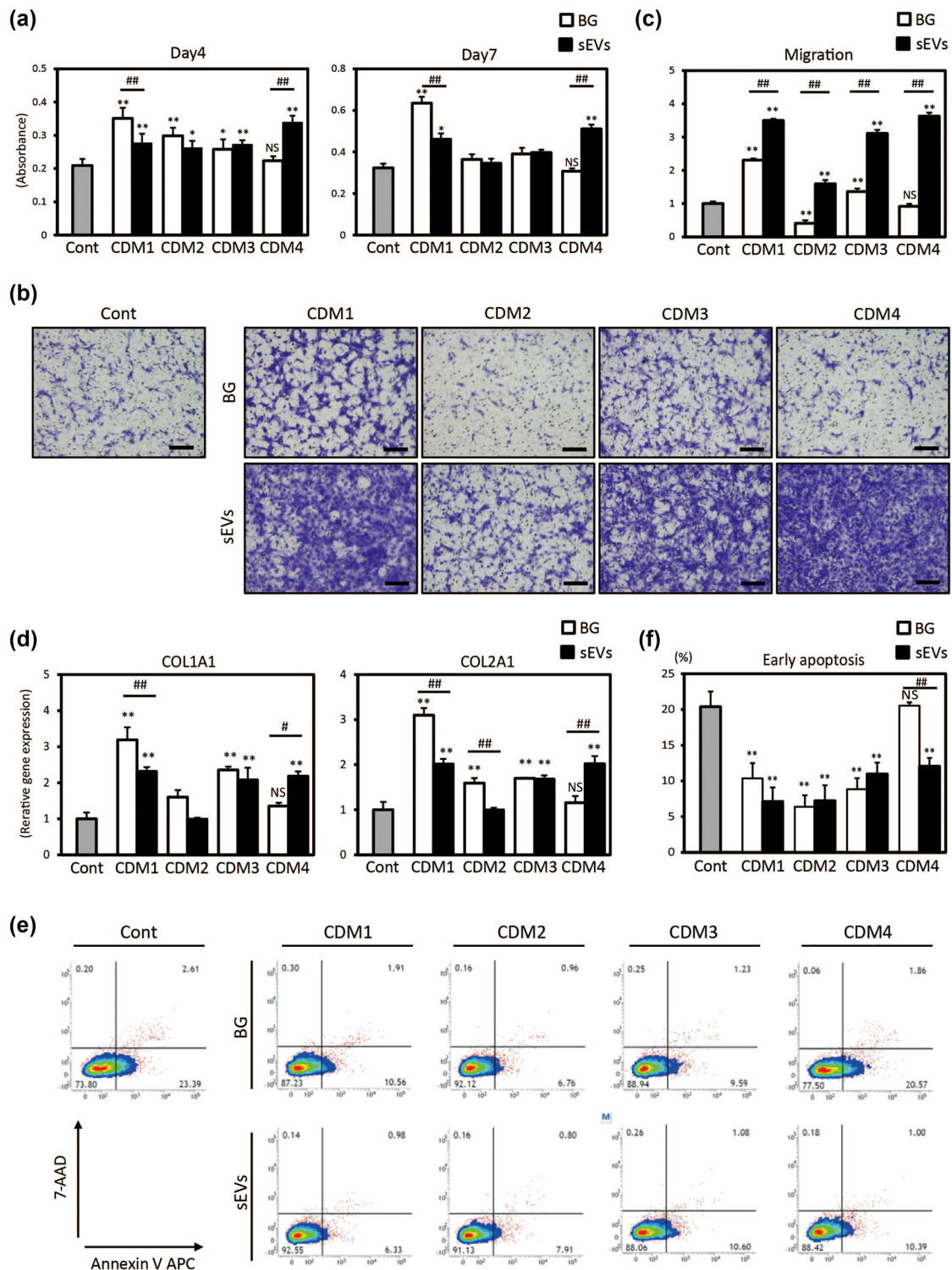


FIGURE 5 The biological effect of each medium-derived sEVs and BG regarding proliferation, migration, ECM synthesis and anti-apoptosis for hACs. Each medium derived sEVs or corresponding BG, or vehicle control (PBS) were added to the cultured hACs at the same particle concentration for each sEVs or the equivalent volume for each BG or control. (a) Cell proliferation assay evaluated on day 4 and 7. $n = 6$. (b, c) Stained microscopic images of the migrated cells and their relative number. The values are shown relative to the control. Three fields were randomly selected per each group. Scale bar: 200 μm . (d) Gene expression analysis by quantitative PCR. Each gene expression is normalized to ACTB and is shown as relative expression to the control group. $n = 3$. (e, f) Flow cytometry analysis for apoptosis detection and the percentage occupied by Annexin-V (+) 7-AAD (-) cells, which were defined as early apoptosis, was calculated. $n = 3$. *, #: $p < 0.05$, **, ##: $p < 0.01$, as compared to the control or two groups connected by a bar, respectively. NS: not significant, as compared to the control groups.

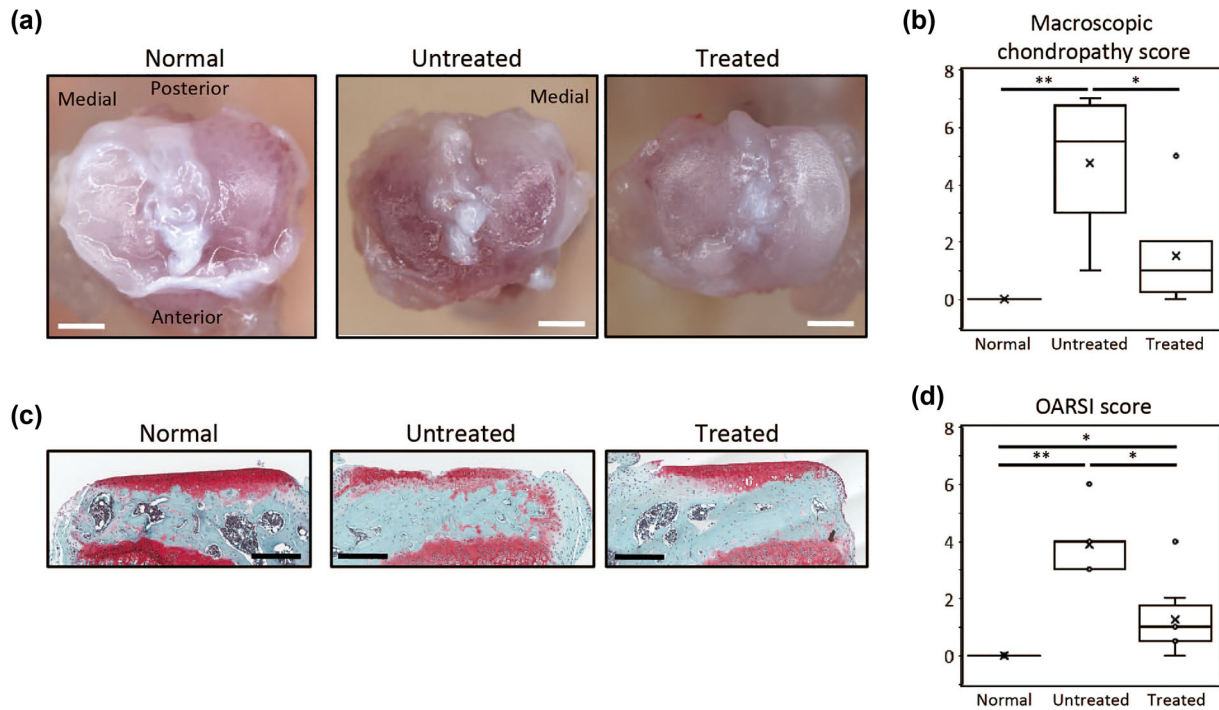


FIGURE 6 The therapeutic effect of CDM4-sEVs on CIOA mice. KOA was induced by the injection of collagenase into the right knee joint and CDM4-sEVs (treated) or CDM4-BG (untreated) were injected at the same site on day 8. Mice were sacrificed on day 28 and the tibias from the injected knee were isolated. Contralateral tibias were used as normal controls (normal). (a, b) Macroscopic images of tibial articular surface and the macroscopic chondropathy scores. Scale bar: 500 μ m. (c, d) Histological sections of the medial aspect of the tibia stained by safranin O and OARSI score. Scale bar: 200 μ m. $n = 5-8$. *: $p < 0.05$, **: $p < 0.01$, as compared between two groups connected by a bar.

CDM4-sEVs group compared with the corresponding BG and the PBS control groups ($p < 0.01$) and there were no significances detected between the CDM4-BG group and the PBS control group ($p = 1.0$) (Figure 4e, f). For the CDM1, 2 and 3 groups, both BG and sEVs significantly suppressed apoptosis compared to the PBS control ($p < 0.01$).

3.6 | Evaluation of the influence of CDM4-sEVs on CIOA mouse in vivo

Based on the results reported above, it was concluded that the CDM4-sEVs samples were the least contaminated by non-sEVs components and the only ones which had clear biological effects on hACs in comparison with their corresponding BG and the PBS controls. Accordingly, CDM4-derived sEVs were tested for their ability to influence the development of osteoarthritis-like pathology in vivo using the CIOA mouse model. The corresponding BG was administered as the control group for these studies. Macroscopic observation at day 28 following administration of the BG samples showed damage to the tibial articular surface with some exposure of subchondral bone with redness (Figure 6a). In contrast, the thickness and whiteness of the articular cartilage was preserved in the animals treated with the sEVs preparations (Figure 6a). Significant differences in the macroscopic chondropathy scores between the BG control group and the treated group were detected ($p < 0.05$) (Figure 6b). Likewise, the histological evaluation revealed that the cartilage on the tibial articular surface had erosive changes with decreased intensity of Safranin O red staining in the BG group. Osteophytes were also detected at the surface edge in the BG control group, while the cartilage maintained its thickness, smoothness and intense Safranin O staining in the animals treated with the sEVs (Figure 6c). The OARSI scores for mice in the treated group were significantly better than those for the BG control group ($p < 0.05$) (Figure 6d).

4 | DISCUSSION

In the present studies, the influence of medium-derived substances was revealed which impacted the potential therapeutic effects of sEVs derived from human ASCs. The sequential isolation methods for sEVs were developed leading to EV with high purity and biological potency, properties that support their potential use in future clinical applications. It was determined that only concentrates of the CDM4-medium contained no detectable particles and proteins, and thus, only sEVs derived from ASCs cultured in CDM4 were of the highest purity compared to other three commercially available and chemically-defined media

that were assessed. The enhanced biological and therapeutic effectiveness of sEVs derived from cells cultured in CDM4 was demonstrated using hACs in vitro and a mouse CIOA model in vivo, when compared to the media controls.

Based on the encouraging results of clinical studies of mesenchymal stromal cell (MSC)-based therapies in osteoarthritis (McIntyre et al., 2018; Yokota et al., 2019), the concept of clinical application of MSC-derived sEVs for treating osteoarthritis (OA) has become an emerging area of research interest. In part, this interest has arisen as sEVs are regarded as one of the potential mode of actions in MSC-based therapies (Hofer & Tuan, 2016). Several preclinical studies have reported the potential feasibility of MSC-sEVs to influence aspects of OA (Cosenza et al., 2017; Woo et al., 2020; Zhang et al., 2018). However, to date there have been no clinical trials with large numbers of patients reported regarding the effectiveness of EV in the treatment of OA.

One of the critical barriers that is required to resolve when contemplating administration of sEVs in clinical settings is the establishment of large-scale production and isolation methods for the sEVs (Gowen et al., 2020). Certainly, sEVs of a similar quality can be generated from MSCs by ultrafiltration and ultracentrifugation methods for in vitro experiments. However, the amount of sEVs obtained by an ultrafiltration method was higher, and without aggregation of the sEVs, in comparison to sEVs obtained by ultracentrifugation (Klymiuk et al., 2019). In addition, it is often difficult to develop a fabrication system for sEVs using ultracentrifugation under current Good Manufacturing Practice (cGMP)-graded controls. Taken together, it may be more reasonable and feasible to use ultrafiltration methods to fabricate sEVs for potential future clinical applications.

When using ultrafiltration methods, exclusion of contaminants in the culture media used during the isolation process should be a key factor. In conventional cell culture, fetal bovine serum (FBS) is widely used as a nutrient to maintain the viability of cultured cells but it has been reported that FBS itself contains sEVs that could affect the recipient cells (Shelke et al., 2014). In this regard, the use of a serum- and xeno-free CDM would be more suitable for the fabrication of clinical grade sEVs preparations. Therefore, we compared four different cGMP compliant, regulatory review/approved serum-free, xeno-free CDMs. CDM 1, 2 and 3 are commercially available media that have been used for expansion of MSCs without losing their multilineage differentiation capacities (cited 2022 July 6th; Lisini et al., 2019; Lindroos et al., 2009). On the other hand, CDM4 media has been recently developed specifically for the isolation of sEVs (Japanese Patent Application No. 2022-154219, CellSource).

The present study provided several findings relevant to the potential clinical application of EV. First, even serum-free, xeno-free CDMs (CDM 1, 2 and 3) had detectable contaminants (particles and proteins), which could not be removed by the tangential flow filtration (TFF) system. Notably, the resultant BG samples from media alone affected the biological activities of hACs, and by extension, also the perceived activities of the sEVs from ASCs expanded in the CDM 1, 2 and 3 media. Thus, in using CDMs (1–3), it is difficult to interpret the changes in biological activity of the resultant hACs as being solely due to the secreted sEVs or also due to the contaminants within the media alone.

In contrast, such contaminants were barely detected or not detected in the CDM4 media. Accordingly, the resultant BG samples obtained with media alone contained no detectable particles, or proteins by silver staining after electrophoresis. Conversely, the sEV samples derived from cells grown in CDM4 contained lipid enclosed particles with a variety of proteins. It was notable that the yields, as well as the purity of the sEVs obtained were significantly higher with CDM4 in comparison with those obtained using CDM 1, 2 or 3. In general, ultrafiltration (UF) is usually followed by a subsequent size-exclusion column (SEC) to increase the purity of the sEVs (Monguio-Tortajada et al., 2019). However, the present study revealed that the isolation method employing ultrafiltration alone and with CDM4 enabled obtaining a high yield and excellent purity of the resulting sEVs, a finding that certainly has a clinically relevant advantage for eliminating the number of steps in the process as well as reducing potential sEVs losses (Nordin et al., 2015). Moreover, the CDM4-sEVs most efficiently promoted the biological activities of cultured hACs in comparison with the other CDM-sEVs. Taken together, it can be concluded that the CDM4 is the best CDM for the purpose of isolating sEVs using only an ultrafiltration protocol among the several CDMs assessed in the present studies. Perhaps most importantly, the administration of CDM4-sEVs significantly suppressed development of osteochondral degradation in vivo in a mouse model of OA, suggesting the suitability of CMD4-derived sEVs interventions for treating osteoarthritis in clinical settings in the future.

While the EV derived from CDM4 were shown to be very effective, one lingering issue is what the particles are that appear to be in CDM1-3 and where they come from. The shape of the particles is somewhat unique, and future research efforts should not only continue to monitor their presence in reagents for use in the preparation of EV for clinical applications, but also where they come from and what their make-up is in more complete detail. Similarly, the finding of proteins not from the donor cells should also be pursued and monitored. Care to make sure such “contaminates” are not present in future studies will also remove potentially confounding factors in the assessment of EV safety and efficacy.

The present study also has some limitations. Considering potential clinical applications, further improvements in obtaining higher yields of sEVs will likely be required based on the different between the in vitro environment and that in the human joint space. Although the production of sEVs is limited from cells grown in 2D culture dishes, changing the culture conditions such as to a microcarrier-based 3D culture systems, may make larger-scale EV production more feasible, and such further improvements should be investigated (Haraszti et al., 2018). Second, the exact mechanisms and detailed signaling cascades mediated by sEVs in the hACs and the knee joint were not fully elucidated in the present study. Therefore, further research is needed to clarify the mode of action of sEVs devoid of media contaminants both in vitro and in vivo. Regarding this point, we assessed the effect of sEVs using only one human chondrocyte population, and only a limited set of in vitro cell activities. In fact, it will be important

to evaluate the therapeutic effect of such EV preparations, such as their anti-inflammatory potential regarding appropriate target cells (not only chondrocytes but also macrophages) in the pro-inflammatory environment, the induction of anabolic events, and repression of catabolic processes. It has been reported that sEVs could target various cells within OA lesions and affect many functions of the cells (Ni et al., 2020). The present study did show that the yield and purity of sEVs correlated with the promotion of several activities of hACs. Moreover, CDM4-derived sEVs demonstrated significant chondro-protective effects compared to the media control in vivo using a mouse CIOA model. In this regard, assessment of the cellular activities tested in the present study using hACs could be a useful option for screening the capacity of sEVs needed for the clinical treatment of OA. The optimal clinical dosage and potential toxicities upon repeated administration of sEVs is another issue that needs to be investigated to enhance the potential success of future clinical applications of EV. While the protein and miRNA distributions assessed in this study resulted in similar properties between the three donors assessed (Figures S2, S3), further study needs to examine the potential differences related to therapeutic efficacy between donors. Despite these limitations, this is the first study to demonstrate the importance of eliminating contaminants in CDM to optimize the purity and efficacy of EVs for therapeutic purposes. Furthermore, a newly developed CDM4, could be a promising media for clinical applications using sEVs therapies targeting various diseases including OA.

5 | CONCLUSIONS

In the present study, the potential risk of contaminants in culture media that affect the purity and capacity of isolated ASC-derived sEVs was demonstrated. The use of a contaminant (particles and protein)-free chemically-defined media leads to the isolation of highly pure sEVs with an enhanced capacity for biological and therapeutic effects in future clinical applications.

AUTHOR CONTRIBUTIONS

Hiroto Hanai: Conceptualization; Data curation; Formal analysis; Investigation; Methodology; Validation; Visualization; Writing—original draft. David A. Hart: Writing—review & editing. George Jacob: Writing—review & editing. Kazunori Shimomura: Writing—review & editing. Wataru Ando: Writing—review & editing. Yusuke Yoshioka: Methodology; Writing—review & editing. Takahiro Ochiya: Supervision; Writing—review & editing. Shinichi Nakagawa: Writing—review & editing. Masato Nakamura: Writing—review & editing. Seiji Okada: Writing—review & editing. Norimasa Nakamura: Conceptualization; Funding acquisition; Project administration; Resources; Software; Supervision; Writing—review & editing.

ACKNOWLEDGEMENTS

The authors would like to thank Center for Medical Research and Education, Graduate School of Medicine, Osaka University for using the Chemi Doc Touch device, the Center for Supporting Drug Discovery and Life Science Research Graduate School of Pharmaceutical Sciences, Osaka University for using the EnVision device and the Immunology Frontier Research Center, Osaka University for using the NanoSight LM10 equipment. This research was partially supported by Platform Project for Supporting Drug Discovery and Life Science Research (Basis for Supporting Innovative Drug Discovery and Life Science Research (BINDS)) from AMED under Grant Number JP21am0101084. The authors also would like to thank Takuo Yamaki for his technical support. This study was supported by a Grant-in-Aid for Scientific Research (B), the Japan Society for the Promotion of Science (Grant Number JP19H03781 and JP22H03201; to NN), AMED under Grant Number JP22mk0101218.

CONFLICT OF INTEREST STATEMENT

This study was supported by joint research support from CellSource (Tokyo, Japan). CellSource did not participate in the performance of the studies or the preparation of the manuscript.

DATA AVAILABILITY STATEMENT

The original contributions presented in the study are included in the article/supplementary material, further inquiries can be directed to the corresponding author.

PATIENT CONSENT STATEMENT

Written informed consent to participate in this study was provided by the participants' legal guardian/next of kin.

ORCID

Hiroto Hanai  <https://orcid.org/0000-0001-5549-005X>

David A. Hart  <https://orcid.org/0000-0001-8580-294X>

George Jacob  <https://orcid.org/0000-0003-0744-1469>

Kazunori Shimomura  <https://orcid.org/0000-0001-8931-146X>

Wataru Ando  <https://orcid.org/0000-0002-9352-465X>

Takahiro Ochiya  <https://orcid.org/0000-0002-0776-9918>
 Shinichi Nakagawa  <https://orcid.org/0000-0003-4789-8068>
 Seiji Okada  <https://orcid.org/0000-0002-5107-8209>
 Norimasa Nakamura  <https://orcid.org/0000-0001-5631-4912>

REFERENCES

- [cited 2022 July 6th]; Available from: <https://kohjin-bio.jp/product/kbm-adsc-4%ef%bc%88serum-free-medium%ef%bc%89/>
- Caplan, A. I., & Dennis, J. E. (2006). Mesenchymal stem cells as trophic mediators. *Journal of Cellular Biochemistry*, 98(5), 1076–1084.
- Cosenza, S., Ruiz, M., Toupet, K., Jorgensen, C., & Noël, D. (2017). Mesenchymal stem cells derived exosomes and microparticles protect cartilage and bone from degradation in osteoarthritis. *Scientific Report*, 7(1), 16214.
- Domini, M., Le Blanc, K., Mueller, I., Slaper-Cortenbach, I., Marini, F. C., Krause, D. S., Deans, R. J., Keating, A., Prockop, D. J., & Horwitz, E. M. (2006). Minimal criteria for defining multipotent mesenchymal stromal cells. The International Society for Cellular Therapy position statement. *Cytotherapy*, 8(4), 315–317.
- Doyle, L., & Wang, M. (2019). Overview of extracellular vesicles, their origin, composition, purpose, and methods for exosome isolation and analysis, *Cells*, 8(7), 727.
- Glasson, S. S., Chambers, M. G., Van Den Berg, W. B., & Little, C. B. (2010). The OARSI histopathology initiative – Recommendations for histological assessments of osteoarthritis in the mouse. *Osteoarthritis and Cartilage*, 18(3), S17–S23.
- Gowen, A., Shahjin, F., Chand, S., Odegaard, K. E., & Yelamanchili, S. V. (2020). Mesenchymal stem cell-derived extracellular vesicles: Challenges in clinical applications. *Frontiers in Cell Developmental Biology*, 8, 149.
- Guingamp, C., Gegout-Pottie, P., Philippe, L., Terlain, B., Netter, P., & Gillet, P. (1997). Mono-iodoacetate-induced experimental osteoarthritis: a dose-response study of loss of mobility, morphology, and biochemistry. *Arthritis Rheumatoid*, 40(9), 1670–1679.
- Gupta, S., Hawker, G. A., Laporte, A., Croxford, R., & Coyte, P. C. (2005). The economic burden of disabling hip and knee osteoarthritis (OA) from the perspective of individuals living with this condition. *Rheumatology*, 44(12), 1531–1537.
- Hanai, H., Jacob, G., Nakagawa, S., Tuan, R. S., Nakamura, N., & Shimomura, K. (2020). Potential of soluble decellularized extracellular matrix for musculoskeletal tissue engineering – Comparison of various mesenchymal tissues. *Frontiers in Cell Developmental Biology*, 8, 581972.
- Haraszti, R. A., Miller, R., Stoppato, M., Sere, Y. Y., Coles, A., Didiot, M.-C., Wollacott, R., Sapp, E., Dubuke, M. L., Li, X., Shaffer, S. A., Difiglia, M., Wang, Y., Aronin, N., & Khvorova, A. (2018). Exosomes produced from 3D cultures of MSCs by tangential flow filtration show higher yield and improved activity. *Molecular Therapy*, 26(12), 2838–2847.
- Hart, D. A., Werle, J., Robert, J., & Kania-Richmond, A. (2021). Long wait times for knee and hip total joint replacement in Canada: An isolated health system problem, or a symptom of a larger problem? *Osteoarthritis and Cartilage Open*, 3(2), 100141.
- Hofer, H. R., & Tuan, R. S. (2016). Secreted trophic factors of mesenchymal stem cells support neurovascular and musculoskeletal therapies. *Stem Cell Research and Therapy*, 7(1), 131.
- Huang, Y., Fu, Z., Dong, W., Zhang, Z., Mu, J., & Zhang, J. (2018). Serum starvation-induces down-regulation of Bcl-2/Bax confers apoptosis in tongue coating-related cells in vitro. *Molecular Medicine Reports*, 17(4), 5057–5064.
- James, S. L., Abate, D., Abate, K. H., Abay, S. M., Abbafati, C., Abbasi, N., Abbastabar, H., Abd-Allah, F., Abdela, J., Abdelalim, A., Abdollahpour, I., Abdulkader, R. S., Abebe, Z., Abera, S. F., Abil, O. Z., Abraha, H. N., Abu-Raddad, L. J., Abu-Rmeileh, N. M. E., Accrombessi, M. M. K., ... Murray, C. J. L. (2018). Global, regional, and national incidence, prevalence, and years lived with disability for 354 diseases and injuries for 195 countries and territories, 1990–2017: A systematic analysis for the Global Burden of Disease Study 2017. *The Lancet*, 392(10159), 1789–1858.
- Katsuda, T., & Ochiya, T. (2015). Molecular signatures of mesenchymal stem cell-derived extracellular vesicle-mediated tissue repair. *Stem Cell Research Therapy*, 6, 212.
- Kim, J. Y., Rhim, W.-K., Yoo, Y. I., Kim, D.-S., Ko, K.-W., Heo, Y., Park, C. G., & Han, D. K. (2021). Defined MSC exosome with high yield and purity to improve regenerative activity. *Journal of Tissue Engineering*, 12, 204173142110086.
- Klymiuk, M. C., Balz, N., Elashry, M. I., Heilmann, M., Wenisch, S., & Arnhold, S. (2019). Exosomes isolation and identification from equine mesenchymal stem cells. *BMC Veterinary Research*, 15(1), 42.
- Kuyinu, E. L., Narayanan, G., Nair, L. S., & Laurencin, C. T. (2016). Animal models of osteoarthritis: Classification, update, and measurement of outcomes. *Journal of Orthopaedic Surgery and Research*, 11, 19.
- Li, J., Lee, Y., Johansson, H. J., Mäger, I., Vader, P., Nordin, J. Z., Wiklander, O. P. B., Lehtiö, J., Wood, M. J. A., & Andaloussi, S. E. (2015). Serum-free culture alters the quantity and protein composition of neuroblastoma-derived extracellular vesicles. *Journal of Extracellular Vesicles*, 4, 26883.
- Lindroos, B., Boucher, S., Chase, L., Kuokkanen, H., Huhtala, H., Haataja, R., Vemuri, M., Suuronen, R., & Miettinen, S. (2009). Serum-free, xeno-free culture media maintain the proliferation rate and multipotentiality of adipose stem cells in vitro. *Cytotherapy*, 11(7), 958–972.
- Lisini, D., Nava, S., Pogliani, S., Avanzini, M. A., Lenta, E., Bedini, G., Mantelli, M., Pecciarini, L., Croce, S., Boncoraglio, G., Maccario, R., Parati, E. A., & Frigerio, S. (2019). Adipose tissue-derived mesenchymal stromal cells for clinical application: An efficient isolation approach. *Current Research in Translational Medicine*, 67(1), 20–27.
- Lopa, S., Colombini, A., Moretti, M., & De Girolamo, L. (2019). Injective mesenchymal stem cell-based treatments for knee osteoarthritis: From mechanisms of action to current clinical evidences. *Knee Surgery, Sports Traumatology, Arthroscopy*, 27(6), 2003–2020.
- Losina, E., Paltiel, A. D., Weinstein, A. M., Yelin, E., Hunter, D. J., Chen, S. P., Klara, K., Suter, L. G., Solomon, D. H., Burbine, S. A., Walensky, R. P., & Katz, J. N. (2015). Lifetime medical costs of knee osteoarthritis management in the United States: Impact of extending indications for total knee arthroplasty. *Arthritis Care Res (Hoboken)*, 67(2), 203–215.
- Maiolo, D., Paolini, L., Di Noto, G., Zandrini, A., Berti, D., Bergese, P., & Ricotta, D. (2015). Colorimetric nanoplasmonic assay to determine purity and titrate extracellular vesicles. *Analytical Chemistry*, 87(8), 4168–4176.
- Maumus, M., Jorgensen, C., & Noël, D. (2013). Mesenchymal stem cells in regenerative medicine applied to rheumatic diseases: Role of secretome and exosomes. *Biochimie*, 95(12), 2229–2234.
- Maumus, M., Roussignol, G., Toupet, K., Penarier, G., Bentz, I., Teixeira, S., Oustric, D., Jung, M., Lepage, O., Steinberg, R., Jorgensen, C., & Noël, D. (2016). Utility of a mouse model of osteoarthritis to demonstrate cartilage protection by IFN γ -primed equine mesenchymal stem cells. *Frontiers in Immunology*, 7, 392.

- McIntyre, J. A., Jones, I. A., Han, B., & Vangsness, C. T. (2018). Intra-articular mesenchymal stem cell therapy for the human joint: A systematic review. *The American Journal of Sports Medicine*, 46(14), 3550–3563.
- Mongiù-Tortajada, M., Gálvez-Montón, C., Bayes-Genis, A., Roura, S., & Borràs, F. E. (2019). Extracellular vesicle isolation methods: rising impact of size-exclusion chromatography. *Cellular and Molecular Life Sciences*, 76(12), 2369–2382.
- Ng, J., Little, C. B., Woods, S., Whittle, S., Lee, F. Y., Gronthos, S., Mukherjee, S., Hunter, D. J., & Worthley, D. L. (2020). Stem cell-directed therapies for osteoarthritis: The promise and the practice. *Stem Cells*, 38(4), 477–486.
- Ni, Z., Zhou, S., Li, S., Kuang, L., Chen, H., Luo, X., Ouyang, J., He, M., Du, X., & Chen, L. (2020). Exosomes: Roles and therapeutic potential in osteoarthritis. *Bone Research*, 8, 25.
- Nordin, J. Z., Lee, Y., Vader, P., Mäger, I., Johansson, H. J., Heusermann, W., Wiklander, O. P. B., Hällbrink, M., Seow, Y., Bultema, J. J., Gilthorpe, J., Davies, T., Fairchild, P. J., Gabrielsson, S., Meisner-Kober, N. C., Lehtiö, J., Smith, C. I. E., Wood, M. J. A., & Andaloussi, S. E. (2015). Ultrafiltration with size-exclusion liquid chromatography for high yield isolation of extracellular vesicles preserving intact biophysical and functional properties. *Nanomedicine*, 11(4), 879–883.
- OARSI White Paper- OA as a Serious Disease. [cited 2022 Feb. 16]; Available from: <https://www.oarsi.org/education/oarsi-resources/oarsi-white-paper-oa-serious-disease>
- Shelke, G. V., Lässer, C., Ghossein, Y. S., & Lötvall, J. (2014). Importance of exosome depletion protocols to eliminate functional and RNA-containing extracellular vesicles from fetal bovine serum. *Journal of Extracellular Vesicles*, 3, 24783.
- Ståhl, A.-L., Johansson, R., Mossberg, M., Kahn, R., & Karpman, D. (2019). Exosomes and microvesicles in normal physiology, pathophysiology, and renal diseases. *Pediatric Nephrology*, 34(1), 11–30.
- Tateiwa, D., Kaito, T., Hashimoto, K., Okada, R., Kodama, J., Kushioka, J., Bal, Z., Tsukazaki, H., Nakagawa, S., Ukon, Y., Hirai, H., Tian, H., Alferiev, I., Chorny, M., Otsuru, S., Okada, S., & Iwamoto, M. (2022). Selective retinoic acid receptor gamma antagonist 7C is a potent enhancer of BMP-induced ectopic endochondral bone formation. *Frontiers in Cell and Developmental Biology*, 10, 802699.
- Théry, C., Boussac, M., Véron, P., Ricciardi-Castagnoli, P., Raposo, G., Garin, J., & Amigorena, S. (2001). Proteomic analysis of dendritic cell-derived exosomes: A secreted subcellular compartment distinct from apoptotic vesicles. *Journal of Immunology*, 166(12), 7309–7318.
- Théry, C., Witwer, K. W., Aikawa, E., Alcaraz, M. J., Anderson, J. D., Andriantsitohaina, R., Antoniou, A., Arab, T., Archer, F., Atkin-Smith, G. K., Ayre, D. C., Bach, J.-M., Bachurski, D., Baharvand, H., Balaj, L., Baldacchino, S., Bauer, N. N., Baxter, A. A., Bebawy, M., ... Zuba-Surma, E. K. (2018). Minimal information for studies of extracellular vesicles 2018 (MISEV2018): A position statement of the International Society for Extracellular Vesicles and update of the MISEV2014 guidelines. *Journal of Extracellular Vesicles*, 7(1), 1535750.
- Toh, W. S., Foldager, C. B., Pei, M., & Hui, J. H. P. (2014). Advances in mesenchymal stem cell-based strategies for cartilage repair and regeneration. *Stem Cell Reviews*, 10(5), 686–696.
- Woo, C. H., Kim, H. K., Jung, G. Y., Jung, Y. J., Lee, K. S., Yun, Y. E., Han, J., Lee, J., Kim, W. S., Choi, J. S., Yang, S., Park, J. H., Jo, D.-G., & Cho, Y. W. (2020). Small extracellular vesicles from human adipose-derived stem cells attenuate cartilage degeneration. *Journal of Extracellular Vesicles*, 9(1), 1735249.
- Woodell-May, J. E., & Sommerfeld, S. D. (2020). Role of inflammation and the immune system in the progression of osteoarthritis. *Journal of Orthopaedic Research*, 38(2), 253–257.
- Yokota, N., Hattori, M., Ohtsuru, T., Otsuji, M., Lyman, S., Shimomura, K., & Nakamura, N. (2019). Comparative clinical outcomes after intra-articular injection with adipose-derived cultured stem cells or noncultured stromal vascular fraction for the treatment of knee osteoarthritis. *The American Journal of Sports Medicine*, 47(11), 2577–2583.
- Yoshioka, Y., Kosaka, N., Konishi, Y., Ohta, H., Okamoto, H., Sonoda, H., Nonaka, R., Yamamoto, H., Ishii, H., Mori, M., Furuta, K., Nakajima, T., Hayashi, H., Sugisaki, H., Higashimoto, H., Kato, T., Takeshita, F., & Ochiya, T. (2014). Ultra-sensitive liquid biopsy of circulating extracellular vesicles using ExoScreen. *Nature Communications*, 5, 3591.
- Zaborowski, M. P., Balaj, L., Breakefield, X. O., & Lai, C. P. (2015). Extracellular vesicles: Composition, biological relevance, and methods of study. *Bioscience*, 65(8), 783–797.
- Zhang, S., Chuah, S. J., Lai, R. C., Hui, J. H. P., Lim, S. K., & Toh, W. S. (2018). MSC exosomes mediate cartilage repair by enhancing proliferation, attenuating apoptosis and modulating immune reactivity. *Biomaterials*, 156, 16–27.

SUPPORTING INFORMATION

Additional supporting information can be found online in the Supporting Information section at the end of this article.

How to cite this article: Hanai, H., Hart, D. A., Jacob, G., Shimomura, K., Ando, W., Yoshioka, Y., Ochiya, T., Nakagawa, S., Nakamura, M., Okada, S., & Nakamura, N. (2023). Small extracellular vesicles derived from human adipose-derived mesenchymal stromal cells cultured in a new chemically-defined contaminate-free media exhibit enhanced biological and therapeutic effects on human chondrocytes in vitro and in a mouse osteoarthritis model. *Journal of Extracellular Vesicles*, 12, e12337. <https://doi.org/10.1002/jev2.12337>